Validation of Synthetic Storm Technique for Rain Attenuation Prediction Over High-Rainfall Tropical Region

Swastika Chakraborty, *Senior Member, IEEE*, Pooja Verma, Bishal Paudel, *Student Member, IEEE*, Ashish Shukla, and Saurabh Das, *Senior Member, IEEE*

***Abstract*— Validation of synthetic storm technique (SST) has been done for prediction of attenuation due to rain over a hilly, high-rainfall, tropical location, Shillong (25°N, 91°E), India. In this letter, considering one year of rain attenuation and rain rate data shows that SST predicted attenuation overestimates while comparing the available experimental result. Storm speed has been found to have no significant effect on the attenuation prediction by SST. Second-order rain attenuation prediction, i.e., prediction of fade slope, has also been studied. Fade slope is found to have been overestimated by SST for all categories of rain events at 20.2- and 30.3-GHz frequency. Exceedance plot of fade duration by SST shows an overestimation for higher frequency and underestimation for lower frequency.**

***Index Terms*— Complementary cumulative distribution function (CCDF), slant path, synthetic storm technique (SST), tropical high rainfall region.**

I. Introduction

RELIABILITY on satellite communication (SATCOM) link above 10 GHz is an important issue for high-rainfall tropical regions. Unavailability of experimental measurement at those frequencies is a major problem for reliable SATCOM link design process. Synthetic storm technique (SST) is found to be very useful to predict rain attenuation time series from rain rate time series in such situation.

The frozen storm hypothesis [1] is used with constant rain speed approximation for conversion of time into distance and used for the calculation of attenuation at a particular time instant. Initially, the theoretical model [2] of SST has been conceptualized and tested against the CCIR database. SST has been tested in three temperate locations in Italy [3] for rain attenuation time series prediction from rain rate time series using long-term measurement of 11.6-GHz beacon signal from SIRIO satellite at 12° elevation angle and circular polarization. The model did not show much bias with respect to the latitude of the location, operating frequency, and attenuation. It has been successfully used in deriving reliable long-term rain attenuation complementary cumulative distribution function (CCDF) [4] and for finding differential equation [5] linking rain attenuation to rain rate over Spino d' Adda. SST was found to perform satisfactorily over several other temperate locations [6], [7] and tropical locations [8]. Recently, modification of SST model named enhanced SST (E-SST) has been shown [9] to have improved prediction for satellite link at EHF frequency band over the temperate climate of Italy for both direct and frequency scaling of attenuation.

Second-order rain attenuation, i.e., fade slope [10] and fade duration [11], was also predicted using SST over tropical location Malaysia [12], and results were compared with ITU-R model predicted rain attenuation and also with the actual measurements. SST was found to outperform ITU-R model for fade duration prediction. However, for fade slope prediction, performance of both models was found to be similar. Over tropical region Nigeria [13], performance of SST has been studied by estimating fade margin, diurnal, seasonal, and annual rain attenuation statistics.

The performance evaluation over tropical regions and especially high-rainfall regions are, however, still inadequate, particularly at Ka-band frequencies. In this letter, the SST is evaluated for 20.2- and 30.3-GHz satellite link at Shillong, which has an average annual rain accumulation of ∼3385 mm.

II. Data and Methodology

A. Experimental Setup

The beacon signals at 20.2 and 30.3 GHz have been received from GSAT-14 satellite at an elevation angle of 58.53° over Umiam, Shillong (25.67°N, 91.92°E) during 2019. Data have been preprocessed for removing sudden spikes and filtered by a Butterworth filter of tenth order to remove the high-frequency components. These high-frequency components generally indicate scintillation and are not included in this letter. Rainfall data have been collected from a collocated laser precipitation monitor (LPM) with 1-min resolution. Wind speed of that location is taken from the Indian meteorological department website [14].

Manuscript received January 21, 2021; revised February 26, 2021 and March 17, 2021; accepted March 18, 2021. Date of publication April 2, 2021; date of current version December 15, 2021. This work was supported in part by the DST-INSPIRE Faculty Scheme and in part by the ISRO- RESPOND Program. *(Corresponding author: Saurabh Das.)*

Swastika Chakraborty, Pooja Verma, and Bishal Paudel are with the Electronics and Communication Engineering Department, Sikkim Manipal Institute of Technology, Gangtok 737136, India.

Ashish Shukla is with the Space Applications Centre, Indian Space Research Organization, Ahmedabad 380015, India.

Saurabh Das is with the Department of Astronomy, Astrophysics and Space Engineering, IIT Indore, Indore 452017, India (e-mail: das.saurabh01@gmail.com).

Digital Object Identifier 10.1109/LGRS.2021.3068334

TABLE I
FREQUENCY-DEPENDENT PARAMETERS

Frequency (GHz)	K_A	α_A	K_B	α_B
20.2	0.09164	1.0568	0.09611	0.9847
30.3	0.2403	0.9485	0.2291	0.9129

B. SST Model

SST fundamentally converts time series of rain rate into time series of rain attenuation in the following way.

Specific attenuation at a point x [15] is given by

$$\Upsilon(x) = kR^{\alpha}(x) \tag{1}$$

where R is the rate of rain at x, and k and α are frequency-dependent parameters. These are separately calculated for the rain layer (A) and melting layer (B) for the frequencies 20.2 and 30.3 GHz [16], [17]. The values are listed in Table I.

Here, the temperatures A and B layers are at 20 °C and 0 °C, respectively.

Rain cell advection velocity v is instrumental in conversion of rain rate time series into attenuation by the relation

$$x = vt. \tag{2}$$

Total attenuation considering the contribution from both the layers can be formulated as [2]

$$A(x) = k_A \int_0^{L_A} R^{\alpha_A}(x + \Delta x \cdot \xi) d\xi + k_B r^{\alpha_\beta} \int_{L_A}^{L_B} R^{\alpha_B}(x, \xi) d\xi. \tag{3}$$

Here ξ is the slant path coordinate, L_A and L_B are the radio path lengths to be calculated from the height of two layers discussed above, altitude of the station, and elevation angle. Δx is the deviation due to the presence of rain layer plus melting layer.

Altitude of the earth station Shillong is

$$H_s = 1525\ 0. \tag{4}$$

Height of two layers A and B in Km is given by

$$H_A = H_B(\varphi) - h. \tag{5}$$

φ is the latitude of Shillong and the melting layer height h is 400 m [3]

$$H_B = 5 \text{ for } \varphi < 23°.$$

And

$$H_B = 5 - 0.075(\varphi - 23) \text{ for } \varphi \geq 23°. \tag{6}$$

Therefore, $H_B(\varphi)$ in our case is 4799 m. It is to be noted that rain height can also be obtained from ITU [18] and turns out to be 4649 m for Shillong.

From (5) and (6)

$$H_A = 4799 - 400 = 4399.8 \text{ m}. \tag{7}$$

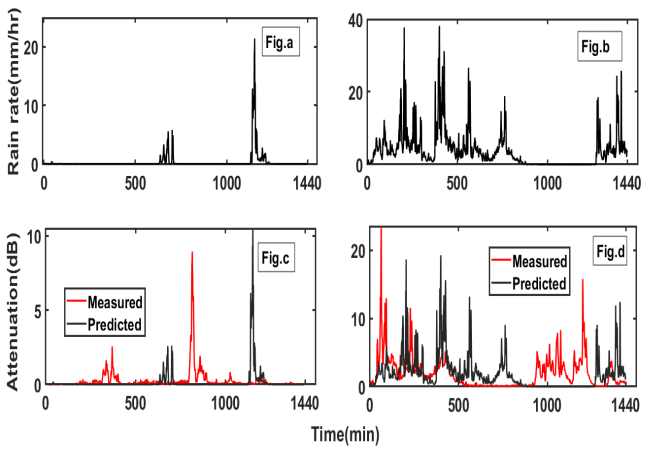

Fig. 1. Measured rain rate time series of (a) July 7, 2019, and (b) October 7, 2019. Corresponding rain attenuation measured as well predicted by SST is shown for (c) July 7, 2019, and (d) October 7, 2019.

Therefore, radio path length for this case is

$$L_A = \frac{H_A - H_s}{\sin\theta} = 3.3958 \text{ km} \tag{8}$$

$$L_B = \frac{H_r - H_S}{\sin\theta} = 3.8674 \text{ km} \tag{9}$$

$$L_B - L_A = 0.4717 \text{ km}. \tag{10}$$

III. RESULT

Rain rate is the only input required for the prediction of attenuation through SST. Therefore, a study has been undertaken to separately understand the performance of SST for both high and low rain intensity events. Here a case study of two such rain events, a low rain intensity event of July 7, 2019, and one high rain intensity event of October 7, 2019, is shown in Fig. 1(a) and (b), respectively. Time series of rain attenuation predicted by SST of these two events along with the measured attenuations is shown in Fig. 1(c) and (d) with natural storm speed of this place, 2 m/s at the received frequency of 20.2 GHz. The prediction reflected by SST method from Fig. 1(c) and (d) is considerably acceptable. However, the peak attenuation value of the events differs to some extent.

To understand the performance of SST for different rain intensity events, the available 19 rain events of the year 2019 are studied.

Rain events having maximum rain intensity above 25 mm/h are classified as high rain intensity events and less than 25 mm/h are classified as low rain intensity events. The CCDF of the predicted attenuation for the available ten rain events of low rain intensity and nine rain events of high rain intensity for both 20.2- and 30.3-GHz frequencies is plotted in Fig. 2(a) and (b) and in Fig. 2(c) and (d), respectively. The CCDF of the predicted attenuation for low rain intensity with different wind speeds is plotted in Fig. 3(a)–(d).The CCDF figures indicate the probability that the Y-axis (rain attenuation) value exceeded during the total measurement period.

It can be seen that SST predicted result matches very well with the measured attenuation CCDF for low rain

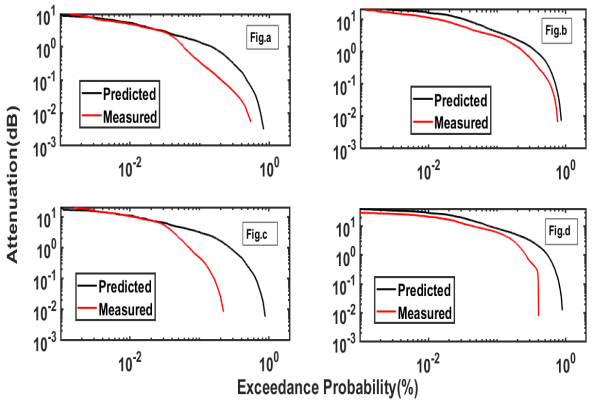

Fig. 2. Comparison of SST and measured CCDF of attenuation with $v = 2$ m/s for the year 2019 at (a) 20.2 GHz for low-intensity rain, (b) 20.2 GHz for high-intensity rain, (c) 30.3 GHz for low-intensity rain, and (d) 30.3 GHz for high-intensity rain.

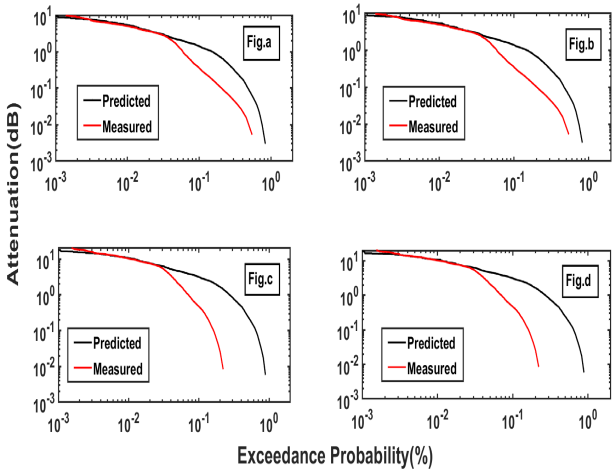

Fig. 3. The CCDF of attenuation for the year 2019 for low-intensity rain with (a) $v = 1$ m/s at 20.2 GHz, (b) $v = 6$ m/s at 20.2 GHz, (c) $v = 1$ m/s at 30.3 GHz, and d) $v = 6$ m/s at 30.3 GHz.

intensity events at low-exceedance probability level. However, the SST significantly overestimates the attenuation for high-exceedance probability values for low-intensity rain events. For high-intensity rain events, however, SST always overestimates the measured attenuation. The difference is more at higher frequency and at higher-exceedance probability level than in other cases. This is summarized in Table II.

The mean square error (MSE) and root mean square error (RMSE) are calculated as

$$\text{MSE} = \frac{1}{n}\sum_{i=1}^{n}(\text{Predited attenuation} - \text{Measured attenuation})^2$$

$$\text{RMSE} = \sqrt{\frac{\sum_{i=1}^{n}(\text{Predited attenuation} - \text{Measured attenuation})^2}{n}}$$

where n indicates the number of data points. The overestimation of rain attenuation by SST for most of the cases can be better explained after analyzing the contribution of melting

TABLE II

QUANTITATIVE PREDICTION ERRORS FOR HIGH AND LOW RAIN INTENSITY EVENTS

Frequency of Operation (GHz)	Rain Type	Error in Prediction (MSE)	RMSE	Standard deviation
20.2	Lower Rain intensity	0.467	0.683	0.386
	Higher Rain intensity	4.97	2.22	1.625
30.3	Lower Rain intensity	0.745	0.863	1.018
	Higher Rain intensity	39.398	6.27	2.905

TABLE III

QUANTITATIVE PREDICTION ERRORS FOR DIFFERENT WIND SPEED

Frequency of Operation (GHz)	Storm Speed(meter/second)	Prediction Error (MSE)	RMSE	Standard deviation
20.2	0.5	0.467	0.682	0.386
	1	0.467	0.685	0.386
	3	0.467	0.682	0.385
	6	0.467	0.683	0.383
	12	0.467	0.683	0.382
30.3	0.5	25.1672	0.863	1.018
	1	0.745	0.863	1.018
	3	0.745	0.862	1.018
	6	0.745	0.862	1.018
	12	0.745	0.864	1.018

layer to rain formation. In this case, the study location belongs to high-rainfall region. According to literature [19], in the period of very high rain rate formation along with high relative humidity, the contribution of melting layer reduces. It reduces due to the significant breakup of melting snowflakes, which result in the reduction of mass weighted melted diameter. This may be the reason for overestimation of rain attenuation by SST in such a location.

To understand the effect of storm speed on the attenuation prediction, the CCDF of the predicted attenuation time series for the frequency 20.2 GHz with the storm speed of 1 and 6 m/s is shown in Fig. 3(a) and (b). Fig. 3(c) and (d) shows the same for 30.3 GHz. Table III shows the errors in prediction for all the cases for different storm speed. It can be noted that there is not much effect of storm speed in time series prediction.

Second-order rain attenuation statistics, such as a fade slope, is also predicted using SST for both low and high rain intensity events in both the frequencies. For fade slope estimation, the time between two successive samples is taken as 1 min. The CCDF of fade slope for both actual and predicted rain attenuation time series for the whole year 2019 is shown in Fig. 4. They are shown separately for each of the rain event categories and for different frequencies. Most of the time, the fade slope for both categories of rain events is

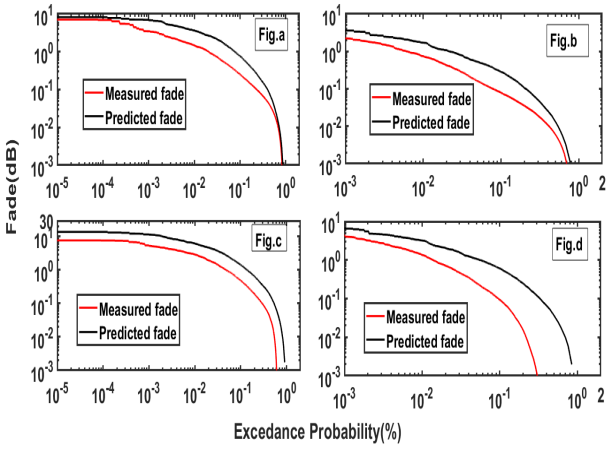

Fig. 4. CCDF of fade slope for (a) $v = 2$ m/s for high rain intensity events at 20.2 GHz throughout the year 2019, (b) $v = 2$ m/s for low rain intensity events at 20.2 GHz throughout the year 2019, (c) $v = 2$ m/s for high rain intensity events at 30.3 GHz throughout the year 2019, and (d) $v = 2$ m/s for low rain intensity events at 30.3 GHz throughout the year 2019.

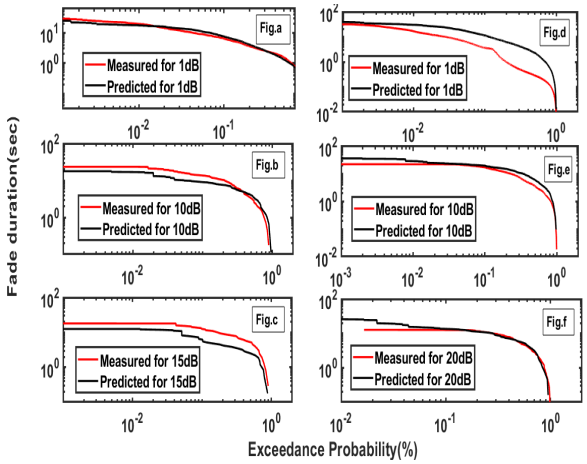

Fig. 5. CCDF of fade duration with $v = 2$ m/s for monsoon month of 2019 at 20.2 GHz for (a) 1-dB threshold, (b) 10-dB threshold, and (c) 15-dB threshold, and at 30.3 GHz for (d) 1-dB threshold, (e) 10-dB threshold, and (f) 20-dB threshold.

overestimated by SST for the frequencies 20.2 and 30.3 GHz, as can be seen from Fig. 4.

Fig. 5 shows the fade duration prediction by SST at 20.2 and 30.3 GHz for different attenuation threshold, considering all the available rain events of the year. The SST technique is found to overestimate the actual observation for duration prediction at higher frequency, whereas it underestimates at lower frequency.

IV. Conclusion

SST is validated in this letter for rain attenuation prediction over a hilly region in India at Ka-band frequencies. Event wise time series prediction shows that the performance of SST technique increases as the operating frequency increases from 20.2 to 30.3 GHz. There is no significant change in prediction performance as the storm speed varies for an event. In case of second-order rain attenuation, i.e., fade slope, the SST overestimates for both categories of rain events at 20.2 and 30.3 GHz. Fade duration is, however, overestimated for higher frequency and underestimated for lower frequency by SST.

Acknowledgment

The authors thankfully acknowledge the scientists of the Space Applications Center, ISRO, for providing the experimental data.

References

[1] G. I. Taylor, "The spectrum of turbulence," *Proc. Roy. Soc. Lond. A, Math. Phys. Eng. Sci.*, vol. 164, no. 919, pp. 476–490, Feb. 1938.

[2] E. Matricciani, "Rain attenuation predicted with a two-layer rain model," *Eur. Trans. Telecommun.*, vol. 2, no. 6, pp. 715–727, Nov. 1991, doi: 10.1002/ett.4460020615.

[3] E. Matricciani, "Physical-mathematical model of the dynamics of rain attenuation based on rain rate time series and a two-layer vertical structure of precipitation," *Radio Sci.*, vol. 31, no. 2, pp. 281–295, Mar. 1996, doi: 10.1029/95rs03129.

[4] E. Matricciani and C. Riva, "The search for the most reliable long-term rain attenuation CDF of a slant path and the impact on prediction models," *IEEE Trans. Antennas Propag.*, vol. 53, no. 9, pp. 3075–3079, Sep. 2005, doi: 10.1109/tap.2005.854539.

[5] E. Matricciani, "A fundamental differential equation that links rain attenuation to the rain rate measured at one point, and its applications in slant paths," in *Proc. 1st Eur. Conf. Antennas Propag.*, Nov. 2006, pp. 1–6, doi: 10.1109/EUCAP.2006.4584792.

[6] D. Nandi, F. Pérez-Fontán, V. Pastoriza-Santos, and F. Machado, "Application of synthetic storm technique for rain attenuation prediction at Ka and Q band for a temperate location, vigo, spain," *Adv. Space Res.*, vol. 66, no. 4, pp. 800–809, Aug. 2020, doi: 10.1016/j.asr.2020.04.046.

[7] E. Matricciani, C. Riva, and L. Castanet, "Performance of the synthetic storm technique in a low elevation 5° slant path at 44.5 GHz in the French Pyrénées," in *Proc. 1st Eur. Conf. Antennas Propag.*, Nov. 2006, pp. 1–6, doi: 10.1109/EUCAP.2006.4584768.

[8] P. Misme and P. Waldteufel, "A model for attenuation by precipitation on a microwave Earth-space link," *Radio Sci.*, vol. 15, no. 3, pp. 655–665, May 1980.

[9] L. Luini, A. Panzeri, and C. G. Riva, "Enhancement of the synthetic storm technique for the prediction of rain attenuation time series at EHF," *IEEE Trans. Antennas Propag.*, vol. 68, no. 7, pp. 5592–5601, Jul. 2020, doi: 10.1109/TAP.2020.2981682.

[10] S. Das, M. Chakraborty, S. Chakraborty, A. Shukla, and R. Acharya, "Experimental studies of Ka band rain fade slope at a tropical location of India," *Adv. Space Res.*, vol. 66, no. 7, pp. 1551–1557, Oct. 2020, doi: 10.1016/j.asr.2020.06.014.

[11] M. Cheffena and C. Amaya, "Prediction model of fade duration statistics for satellite links between 10-50 GHz," *IEEE Antennas Wireless Propag. Lett.*, vol. 7, pp. 260–263, 2008, doi: 10.1109/LAWP.2008.921369.

[12] S. L. Jong, C. Riva, M. D'Amico, H. Y. Lam, M. M. Yunus, and J. Din, "Performance of synthetic storm technique in estimating fade dynamics in equatorial malaysia," *Int. J. Satell. Commun. Netw.*, vol. 36, no. 5, pp. 416–426, Sep. 2018, doi: 10.1002/sat.1246.

[13] J. S. Ojo and O. C. Rotimi, "Diurnal and seasonal variations of rain rate and rain attenuation on Ku-band satellite systems in a tropical region: A synthetic storm techniques approach," *J. Comput. Commun.*, vol. 3, no. 4, pp. 1–9, 2015.

[14] *Indian Meteorological Department*. Accessed: Mar. 22, 2021. [Online]. Available: http://aws.imd.gov.in:8091/

[15] *Propagation Date and Prediction Methods Required for the Design of Earth-Space Telecommunication Systems*, document ITU-R Recommendations P. 618-9, International Telecommunication Union, Geneva Switzerland, 2007.

[16] *Specific Attenuation Model for Rain for Use in Prediction Methods*, document ITU-R Recommendations P. 838-3, International Telecommunication Union, Geneva Switzerland, 2005.

[17] D. Maggiori, "Computed transmission through rain in the 1-400 GHz frequency range for spherical and elliptical drops and any polarization," *Alta Frequenza*, vol. 50, pp. 262–273, Oct. 1981.

[18] *Rain Height Model for Prediction Method*, document ITU-R Recommendations P. 839-4, International Telecommunication Union, Geneva Switzerland, 2013.

[19] K. Mróz, A. Battaglia, S. Kneifel, L. von Terzi, M. Karrer, and D. Ori, "Linking rain into ice microphysics across the melting layer in stratiform rain: A closure study," *Atmos. Meas. Techn.*, vol. 14, no. 1, pp. 511–529, Jan. 2021, doi: 10.5194/amt-14-511-2021.